Biomaterials 34 (2013) 1115–1127

Contents lists available at SciVerse ScienceDirect

Biomaterials

journal homepage: www.elsevier.com/locate/biomaterials

Rapamycin encapsulated in dual-responsive micelles for cancer therapy

Yi-Chun Chen [a], Chun-Liang Lo [b], Yu-Fen Lin [c], Ging-Ho Hsiue [a,c,*]

[a] Department of Chemical Engineering, National Tsing Hua University Hsinchu, Hsinchu 300, Taiwan, ROC
[b] Department of Biomedical Engineering, National Yang Ming University, Taipei 112, Taiwan, ROC
[c] Department of Chemical Engineering and R&D Center for Membrane Technology, Chung Yuan Christian University, Chungli 320, Taiwan, ROC

ARTICLE INFO

Article history:
Received 2 September 2012
Accepted 11 October 2012
Available online 10 November 2012

Keywords:
Polymeric micelles
pH-responsive
Rapamycin
Autophagy
Intracellular drug delivery

ABSTRACT

Rapamycin has been developed as a potential anticancer drug for treatment in rapamycin-sensitive cancer models, but its poor water solubility greatly hampers the application to cancer therapy. This study investigated the preparation, release profiles, uptake and *in vitro*/*in vivo* study of a dual-responsive micellar formulation of rapamycin. Rapamycin-loaded micelles (rapa-micelles) measured approximately ca. 150 nm with narrow size distribution and high stability in bovine serum albumin solution. It was shown that rapamycin could be loaded efficiently in mixed micelles up to a concentration of 1.8 mg/mL by a hot shock protocol. Rapamycin release kinetic studies demonstrated that this type of micellar system could be applied in physiological conditions under varied pH environments. Confocal and pH-topography imaging revealed a clear distribution of rapa-micelles, and visible intracellular pH changes which induced encapsulated rapamycin to be released and then induced autophagolysosome formation. *In vivo* tumor growth inhibition showed that rapa-micelles exhibited excellent antitumor activity and a high rate of apoptosis in HCT116 cancer cells. These results indicated that dual-responsive mixed micelles provided a suitable delivery system for the parenteral administration of drugs with poor water solubility, such as rapamycin, in cancer therapy.

1. Introduction

Rapamycin is a carboxylic lactone-lactam macrolide derived from the bacterium *Streptomyces hygroscopicus* [1]. Rapamycin was originally used as an antifungal agent [1] and was later developed as an approved immunosuppressant [2] and potential anticancer drug [3]. Preclinical data show inhibition of tumor growth in a number of cell lines, including lung [4], cervix [5], colon [6] and breast [7] cell carcinomas. In addition, rapamycin is the most commonly used chemical to induce autophagy. Autophagy is a lysosome-based pathway that describes the degradation and recycling of proteins and intracellular components for maintaining cellular homeostasis. During autophagy, cytoplasm sequestered and then formed double-membraned vesicles which is termed as autophagosomes. Autophagosomes then fuse with lysosomes, containing acid hydrolases, which is called an autophagolysosome [8]. However, autophagy also protects some cancer cells against anticancer treatments by blocking the apoptotic pathway [9]. For cancer therapy, autophagy is associated with functions primarily in tumor suppression by removing possibly growth factors and reduces chromosome instability. Rapamycin is one of the few mammalian Target of Rapamycin (mTOR) inhibitors that specifically target an autophagy-regulatory protein. Autophagy could be a therapeutic target for rapamycin treatment of cancer. A growing volume of evidence supports the hypothesis that mTOR is a kinase that functions as a master switch between catabolic and anabolic metabolism [10]. Consequently, the mTOR pathway determines whether cells—particularly tumor cells—will grow and proliferate. Inhibitor of mTOR, rapamycin, induces cell cycle arrest at the transition from G1-S phase [11,12]. Recent studies have reported a sensitivity of cancer cell lines to the mTOR signaling pathway [5,10,13]. The mechanism behind this anticancer effect is based on the anti-angiogenic properties of rapamycin, which relate to blocking vascular endothelial growth factor (VEGF) production and stimulation of endothelial cells [14,15].

Despite the potency of rapamycin demonstrated in the above studies, the systemic delivery of rapamycin to tumor sites constitutes a major challenge in the field of cancer therapy. Delivery is impeded by rapamycin's poor solubility in water (2.6 μg/mL) [16], and by its low bioavailability [17] and dose-limiting toxicity. To fully exploit the therapeutic potential of rapamycin in systemic administration, the drug carriers should provide a suitable intravenous

* Corresponding author. Department of Chemical Engineering, National Tsing Hua University Hsinchu, Hsinchu 300, Taiwan, ROC. Tel.: +886 3 571 9956; fax: +886 3 572 6825.
E-mail address: ghhsiue@mx.nthu.edu.tw (G.-H. Hsiue).

0142-9612/$ – see front matter © 2012 Elsevier Ltd. All rights reserved.
http://dx.doi.org/10.1016/j.biomaterials.2012.10.034

(iv) formulation, and should be non-cytotoxic, stimuli-responsive, and stable in the circulation. Various investigations have demonstrated that an efficient delivery system stabilizes rapamycin and achieves controlled drug distribution, despite its poor water-solubility. Approaches like successful local drug delivery systems of rapamycin have been used on immunosuppression of the immune system [18,19]. Anticancer therapy using rapamycin has been made possible by advances in the delivery system designed to control the release rate for drugs administered either by injection [20,21] or orally [22,23]. For iv injection, Forrest et al. reported a formulation of rapamycin prepared using poly(ethylene glycol)-*b*-poly(ε-caprolactone) micelles [20]. Lu et al. demonstrated that poly(ethylene glycol)-*b*-poly(2-methyl-2-benzoxycarbonyl-propylene carbonate) copolymer could be used to prepare rapamycin-loaded micelles [21]. However, the carriers did not optimize for the iv formulations of rapamycin because the encapsulated drug was rapidly or sustained released in a neutral environment. After iv injection, a long-circulating drug carrier (10–200 nm) demonstrated significant selective targeting of tumors of a specific size range, and the particle accumulated in solid tumors because of an enhanced permeability and retention effect (EPR effect) [24]. For tumor-specific drug release, carriers can be designed to stabilize under physiological condition and to selectively respond to stimuli near tumor sites, such as minor increases in local temperature [25] or decreases in extracellular pH [26]. Thus, for most anti-cancer drug particulate carriers, the triggering mechanism must occur in the tumor extracellular microenvironment and/or acidic organelles to release the drug into the cytoplasm. The properties of stimuli response for carriers of rapamycin could be designed to favor extracellular or intracellular pH-triggered drug release.

As our previous polymeric micelle systems, dual-responsive micelles from mPEG-*b*-P(HPMA-Lac-*co*-His) (poly(ethylene glycol)-*b*-poly(N-(2-hydroxypropyl) methacrylamide dilactate)-co-(N-(2-hydroxypropyl) methacrylamide-*co*-histidine)) and mPEG-*b*-PLA (poly(ethylene glycol)-*b*-poly(D,L-lactide)) diblock copolymers exhibited a simple, non-toxic property as well as excellent tumor targeting *in vivo* [27]. The current study describes the formulation to improve the solubility of rapamycin for enhanced intracellular delivery and improved antitumor efficacy (Schematic representation in Scheme 1). Hydrophobic interactions of the system are temperature-dependent, thus the efficient use of temperature might provide one method for incorporating drugs with poor water-solubility. This system offers a pH-sensitive structural feature and stability under the neutral serum albumin environment. Rapa-micelles disintegrate because of structural changes in intracellular pH, allowing for the rapid release of the drug from their hydrophobic regions, thus preventing or decreasing leakage of the anticancer drug into systemic circulation, and enhancing the effective concentration of rapamycin. The PEG modified particles are taken up extremely efficiently by a number of different routes [28]. Caveolae represent the main non-clathrin-dependent route from the cell surface to endosomes [29]. This study investigated the encapsulation of rapamycin in dual-responsive micelles by a heat shock protocol, and the stability and pH-dependent release behavior. Intracellular pH topography and cytotoxicity were investigated in human colon cancer HCT116 cells lines and the results were compared with those of free rapamycin. Finally, antitumor therapeutic efficacy and tumor apoptosis of the rapa-micelles and free drug were evaluated in a HCT116 cancer xenograft model.

2. Materials and methods

2.1. Materials

Methoxy poly(ethylene glycol) with Mw 5000 (mPEG) and α-t-butyloxy-carbonylamino-ω-hydroxy-poly(ethylene glycol) (Boc–NH–PEG-OH) with Mw 3000 were purchased from Iris Biotech. D,L-lactide and palladium were purchased from Lancaster. Cy5.5 mono NHS ester was purchased from GE Healthcare, and N-(2-hydroxypropyl) methacrylamide (HPMA) was purchased from Polysciences. 4,4′-Azobis(4-cyanovaleric acid) (ABCPA) and stannous octoate ($Sn(Oct)_2$) were purchased from Aldrich. Sodium hydroxide (NaOH), bovine serum albumin (BSA), potassium chloride (KCl), 2-(*N*-morpholino)ethanesulfonic acid (MES), 4-(2-hydroxyethyl)-1-piperazineethanesulfonic acid (*HEPES*), calcium chloride ($CaCl_2$), and magnesium chloride ($MgCl_2$) were purchased from Sigma. 4-(dimethylamino) pyridine (DMAP), N-(tert-butoxycarbonyl)-L-histidine, and 1-(3-dimethylaminopropyl)-3-ethylcarbodiimide (EDC) were purchased from TCI. Acetonitrile (ACN), dichloromethane (DCM), and ethanol (EtOH) were purchased from TEDIA. Rapamycin (99%) was purchased from LC Laboratories. LysoSensor Blue DND-167, anti-LC3B (against isoform B of human microtubule-associated protein 1 light chain 3) antibody, Alexa Fluor 488, and Carboxyl-seminaphthorhodafluor-1 acetoxymethylester (SNARF-1-AM) was purchased from Invitrogen. Dulbecco's modified Eagle's medium (DMEM) was purchased from GIBCO.

The cell lines of human cervical cancer HeLa, human colon cancer HCT116, and normal human foreskin fibroblast HS68 cells were obtained from the Bioresource

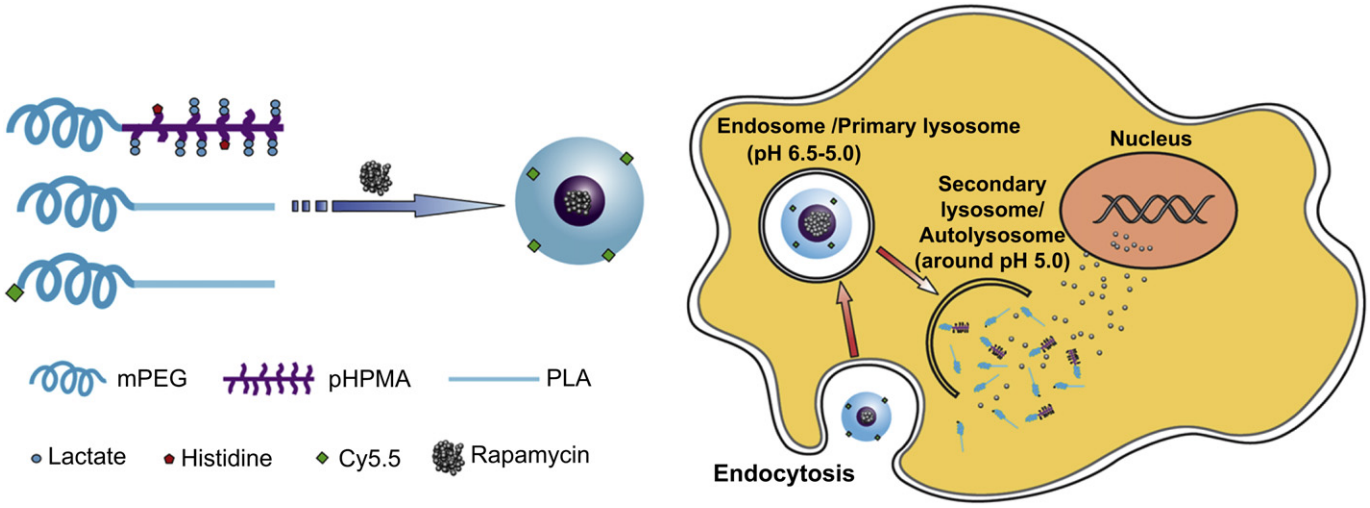

Scheme 1. Schematic representation of mixed micelle composed of the diblock copolymers mPEG-b-P(HPMA-Lac-co-His), mPEG-*b*-PLA and Cy5.5-PEG-PLA and loaded with rapamycin. The dual-responsive drug carrier is designed for the intracellular delivery. The acidic lysosomal compartments could induce the deformation of the rapa-micelles to trigger the release of enclosed drug molecules.

Collection and Research Center, Hsinchu, Taiwan. The HeLa, HS68, and HCT116 cells were maintained in DMEM and McCoy's 5A medium containing L-glutamine (Gibco), 1% penicillin-streptomycin (Gibco), and 10% fetal bovine serum (FBS) (Invitrogen) at 37 °C and 5% CO_2. A viable cell kit based on the compound 3-(4,5-dimethylthiazol-2-yl)-5-(3-carboxymethoxyphenyl)-2-(4-sulfophenyl)-2H-tetrazolium (MTS) was purchased from Promega.

2.2. Preparation of empty and rapamycin-loaded micelle (rapa-micelle)

We synthesized mPEG-*b*-PLA, Cy5.5-PEG-*b*-PLA, and mPEG-*b*-P(HPMA-Lac-co-His) by ring-opening polymerization, and characterized the compounds as previously described [27]. Micelles were prepared by the temperature-dependent phase transition behavior using a modified heat shock protocol. Rapa-micelles were formed by the same procedure as described previously [27]. Rapamycin was dissolved in ethanol in concentrations ranging from 1 to 20 mg/mL. 1 unit of rapamycin solution (0.2 mL) was added slowly to 10 units of a solution comprising mPEG-*b*-P(HPMA-Lac-*co*-His) and mPEG-*b*-PLA (75:25 wt, 2 mL), and stirred at 0 °C. Then the mixture was heated rapidly to 60 °C while being stirred for 1 min, and the ethanol was removed by rotary evaporation at 40 °C. Free rapamycin was removed by filtration through a sterile, surfactant-free, 0.45 μm cellulose acetate filter (Sartorius Stedim). The loading capacity (LC) was calculated using the following formula:

$$\text{Drug content}(\%w/w) = (\text{mass of encapsulated drug})/(\text{mass of encapsulated drug} + \text{mass of polymer in micelle}) \times 100\%$$

The encapsulation efficiency (EE) of the rapa-micelles was calculated using the following formula:

$$\text{Encapsulation efficiency}(\%w/w) = (\text{mass of encapsulated drug})/(\text{mass of initial drug}) \times 100\%$$

2.3. Characterization of rapa-micelles

Dynamic light scattering (DLS) was used to determine the size and size distribution of the micelles. For DLS measurements, the micellar solutions were incubated at 37 °C for 1 h. The average particle size and size distribution of the micelles were determined using a Zetasizer (Malvern-zetasizer 3000HS, Malvern, UK) at an angle of 90° and at 37 °C. The pH of the rapa-micelles solutions was altered by adding 7.5 mM HCl. The correlations among DLS data were analyzed by the constrained regularized CONTIN method. The CONTIN method is particularly useful for analyzing multicomponent systems for DLS data.

To perform transmission electron microscopy (TEM) observations of the micelle size and morphology, we employed a Hitachi H-7650 microscope at an accelerating voltage of 120 kV. A drop of sample solution (ca. 7 μL) with a 2 mg/mL concentration was placed onto a copper grid coated with carbon, tapped with filter paper to remove surface water, and air-dried for 5 min. Then the grid was negatively stained with 2 wt% uranyl acetate solution, tapped with filter paper to remove surface water, and vacuum-dried for 24 h.

2.4. Stability and pH stimulation of rapa-micelles

The stability of the loaded-drug micelles was studied using PBS buffer and serum albumins. In pH 7.4 PBS buffer, the micellar solutions (1 mg/mL) were prepared as described in previous section. The stability of the micelles in the presence of proteins was assessed as described in the followings. Rapa-micelles in pH 7.4 PBS buffer (2 mg/mL) were mixed with an equal volume of 10 wt% BSA dissolved in PBS buffer. The mixture was incubated at 37 °C. The average diameter and polydispersity index (PDI) of the resulting samples were measured by DLS at 37 °C over time, as described in previous section. The average diameter of micelles before treatment with PBS buffer of pH 7.4, 6.5, 6.0, 5.5 or 4.5 was measured to identify pH stimulation.

2.5. Drug release assay

Rapamycin release assay was based on the methodology of Bisht et al. with slight modification [22]. Lyophilized rapa-micelles (100 mg) encapsulating 25 mg of rapamycin were dispersed in 50 mL PBS under three different pH conditions (pH 7.4, 6.0, 5.0), and the solution was divided among microfuge tubes (1 mL/tube). The microfuge tubes were kept in an oven at 37 °C. Free rapamycin is almost insoluble in water (2.6 μg/mL). Thus at predetermined time intervals, the solution was centrifuged at 3000 rpm for 5 min to separate the released rapamycin from the rapa-micelles. Next, the released rapamycin was dissolved in 1 mL of ethanol and the absorbance was measured spectrophotometrically at 273 nm. The concentration of the released rapamycin was then calculated.

2.6. Method of internalization and immunofluorescence

To facilitate cell adhesion, 35 mm glass-bottom culture dishes (MatTek Corporation) were pre-coated with poly-D-lysine. Cell suspensions of HCT116 and HeLa cells (2×10^5 cells in 2 mL) were added to the dishes and incubated overnight at 37 °C under a 5% CO_2 atmosphere. The medium was removed and we then added a Cy5.5-tagged rapa-micellar solution, diluted in medium (ca. 1 μM rapamycin) and supplemented with FBS. The cells were incubated for 1 and 3 h at 37 °C. Each dish was washed with PBS (pH 7.4) three times and loaded with LysoSensor Blue DND-167 for 30 min. After triple washing with PBS, each dish was treated with 1 mL of 4% paraformaldehyde solution for 10 min to fix the cells. The fixed cells were permeabilized with 0.2% Triton X-100 in PBS, then were incubated with anti-LC3B antibody and then labeled with secondary antibodies conjugated with Alexa Fluor 488. and then mounted on a slide for observation. Confocal laser scanning microscopy (CLSM) was performed with a Leica TCS SP5 Confocal Spectral Microscope Imaging System, using excitation wavelengths of 373, 488 and 633 nm and LP filters of 425 ± 10, 520 ± 10 and 695 ± 10 nm to detect LysoSensor, AutophagySensor and Cy5.5, respectively.

2.7. pH topography

Intracellular pH was measured by ratiometric analysis of SNARF-1 fluorescence. We used a modified method based on intracellular pH distribution [30,31]. The HCT116 cells were loaded onto the dishes by the previous description. To measure the intracellular pH, the medium was removed and sample solutions (rapamycin and rapa-micelles) were added; the test solutions were diluted in medium (ca. 1 μM rapamycin) and supplemented with FBS. The cells were incubated for 3 and 24 h at 37 °C under a 5% CO_2 atmosphere. Each dish was washed three times with PBS (pH 7.4) and loaded with pH probe SNARF-1-AM solution (5 μM, 2 mL) for 2 h. The dish was then washed and treated with 1 mL of 4% paraformaldehyde solution for 10 min to fix the cells, then mounted on a slide. The fluorescence ratio of SNARF-1 to intracellular pH was determined by incubating the cells for 5 min with the H^+/K^+ exchange ionophore nigericin (5 μg/mL). Calibration buffers contained in the presence of K^+-containing solutions to equilibrate the endomembrane pH with that of the external medium [32] (125 mM KCl, 10 mM Mes, 10 mM Hepes, 1 mM $CaCl_2$, 1 mM $MgCl_2$). The pH range of calibration buffers was 6.0–7.4 by adding 7.5 mM HCl or NaOH. The ratio of fluorescence intensity of SNARF-1 at 585/640 nm was calibrated in HCT116 cells using calibration buffer adjusted to the desired pH. Fluorescence was observed under a CLSM with an excitation wavelength of 514 nm and two LP filters of 585 ± 10 (channel 1) and 640 ± 10 nm (channel 2), respectively. Signals were scanned simultaneously in both channels and the intensity ratio for channel 1: channel 2 was calculated for each pixel. The intensity ratios were color coded according to a generic color bar, to illustrate the pH topography.

2.8. Cytotoxicity evaluation

The cytotoxicity of each sample was determined by measuring the inhibition of cell growth using a tetrazolium dye (MTS) assay [33]. The HCT116 and HS-68/HeLa cells (5×10^3 cell/mL) harvested in the logarithmic growth phase were seeded on a 96-well plate in McCoy's 5A and DMEM medium with 10% FBS, in a humidified atmosphere of 5% CO_2 at 37 °C. After the cells had been incubated in the logarithmic growth phase, various concentrations of rapamycin were added to samples for 24 and 72 h of co-culturing. At the end of the experiment, MTS assay was conducted and the percentage of viable cells was calculated. In addition, the cytotoxicities of materials were measured using cancer cells and normal human foreskin fibroblast HS68 cells (5×10^3 cell/mL).

2.9. In vivo antitumor activity [26,30]

The tumor model was established as described above. When the transplanted tumor volume reached approximately 50 mm^3 (7 days after inoculation), animals were randomly divided into two groups (experimental and control groups, six animals per group). Free rapamycin was dosed in 4% ethanol/5% PEG 400/5% Tween 80 in water for injection solution [13]. Animals were treated intravenous *via* the tail vein at 4 different time points with an interval of 7 days (days 0, 7, 14 and 21). Mice were injected with 0.2 mL of different formulations of rapamycin solutions (rapa-micelles and free rapamycin at a dose of 15 mg/kg) or neat saline/empty micelles (negative control). Follow-up was performed for 24 days following the administration experiments were performed. During the course of the follow-up, tumor size was measured three times a week using a Vernier's caliper. Tumor volume was calculated as follows: $V = (ab^2)/2$ (where a and b indicate the major and minor axes of the tumor, respectively). Mice body weight (as an indirect indicator of general animal wellness) and clinical status were carefully recorded. To evaluate the antitumor activity, the relative tumor volume was calculated as the ratio of tumor volume on that day to its value at the start of therapy. To evaluate toxicity, we assessed mortality and relative body weight (calculated as the ratio of tumor volume on that day to its value at the start of therapy).

2.10. TUNEL assay

Excised tumors were immediately embedded into OCT medium and snap frozen in dry ice. 4 μm thick sections were prepared with a cryostat and fixed in 4%

paraformaldehyde (EMS, Hatfield, PA) for 20 min at room temperature. After the sections were washed with PBS-Tw (0.3% Tween 20 in PBS at pH = 7.4) three times for 10 min each, the apoptosis cells were stained with ApopTag® Fluorescein *In Situ* Apoptosis Detection Kit S7110 from Chemicon (Billerica, MA) according to the manufacturer's instruction and the nucleus were labeled with DAPI.

3. Results and discussion

3.1. Rapa-micelle preparation

We recently reported on a biodegradable mixed micelle system using poly(ethylene glycol)-*b*-poly(N-(2-hydroxypropyl) methacrylamide dilactate)-*co*-(N-(2-hydroxypropyl) methacrylamide-co-histidine) (mPEG-*b*-P(HPMA-Lac-*co*-His)) diblock copolymer together with a temperature- and pH-responsive, poly(ethylene glycol)-*b*-poly(D,L-lactide) (mPEG-*b*-PLA) diblock copolymer with a low critical micelle concentration (CMC) value [27]. This drug carrier system has been successfully applied to solubilize the hydrophobic anticancer drug doxorubicin. The PEG segment acts as a highly hydrophilic block with excellent biocompatibility that offers stability to the drug carrier, and allows the micelles to avoid recognition by monocytes [34]. The mPEG-*b*-P(HPMA-Lac-*co*-His) copolymer was soluble in aqueous solution below the cloud point (CP), but precipitated at higher temperatures because of temperature-dependent hydrophobic interactions. N-(2-hydroxypropyl) methacrylamide-*co*-histidine was used to provide the pH and hydrophobic moiety. The buffering capacity of histidine ($pK_b = \sim 6.0$) [35]and therefore its imidazole ring of P(HPMA-Lac-*co*-His) segment was protonated in a slightly acidic environment.

Previous research has shown that mPEG-*b*-P(HPMA-Lac-*co*-His) and mPEG-*b*-PLA formed mixed micelles in an aqueous solution, above the solution's CP, and that two copolymers were completely miscible in homogenous cores [27]. The results demonstrated that a 75/25 mass ratio for mPEG-*b*-P(HPMA-Lac-*co*-His) to mPEG-*b*-PLA produced micelles of optimal size and PDI. The mixed micelle system showed an amphiphilic character with a hydrophobic inner core and a hydrophilic outer shell, and displayed a good loading capacity for doxorubicin. In the current study, rapa-micelles were prepared by dissolving rapamycin in ethanol and adding the mixture to an aqueous copolymer solution at 0 °C, then quickly heating it above the CP (60 °C). After filtration through a 0.45 μm filter (to remove rapamycin precipitates), a clear white dispersion was obtained (Fig. S1C and D), demonstrating that rapamycin had been completely dispersed in the aqueous media by the polymeric micelle system. In contrast, when free rapamycin in ethanol was suspended in water, rapid and large precipitation of the hydrophobic rapamycin was observed (Fig. S1A and B). In free rapamycin solution, the concentration of rapamycin (2.8 μg/mL) was almost equal to the solubility of rapamycin in water after 0.45 μm filtration. This simple loading method successfully encapsulated rapamycin and did not make use of large amounts of organic solvents (e.g. tetrahydrofuran [18], acetone [19,20], dichloromethane [21] or chloroform [22]) which are toxic and must be totally removed. The older loading method relies on the use of such solvents.

Fig. 1A shows the loading capacity (LC) and the encapsulation efficiency (EE) of rapa-micelles containing 0.1–2 mg/mL rapamycin and 2 mg/mL copolymers, plotted against rapamycin concentration. We observed that LC increased rapidly from 4.5% (drug concentration 0.1 mg/mL) to approximately 26.0% (drug concentration 1 mg/mL) and then leveled off. The results suggested that not enough copolymers had been added to saturate the rapamycin, resulting in the formation of rapamycin aggregates at high drug concentrations. The EE results indicated that when low amounts of rapamycin were added (0.1–0.5 mg/mL), most drug retained in the micellar solution (81.8–90.2%). With increasing drug concentrations (up to 2 mg/mL), the EE decreased to 26.1%, once again because not enough copolymers were present to solubilize the high concentration of rapamycin; this deficiency resulted in the formation of rapamycin aggregates which could be removed by filtration. Fig. 1B shows a plot of the average diameter and PDI of rapa-micelles against rapamycin concentration. As initial drug concentration was increased, the average rapa-micelle size increased from 77.9 to 257.8 nm and PDI range from 0.41 to 0.21. The PDI of the first three drug concentrations (0.1, 0.2 and 0.4 mg/mL) is between 0.41 and 0.31, we suggest the hydrophobic drug rapamycin can help to be solidified micelles because of the relatively strong physical interactions between copolymer and drug. Moreover, presumably free copolymers rapidly precipitated at low drug concentrations. The PDI data showed a wide range in size distribution at drug concentrations of 1.5 and 2.0 mg/mL; presumably the rest rapidly precipitated at higher concentrations. The results indicated that more rapamycin was encapsulated in mixed micelles (rapamycin concentration lower than 1 mg/mL), resulting in loaded micelles containing more drug per micelle.

Fig. 1C shows the LC and EE of rapa-micelles containing 1.0 mg/mL rapamycin and between 1.0 and 10.0 mg/mL of copolymers, plotted against the copolymer concentration. At this fixed rapamycin concentration (1.0 mg/mL), the LC decreased from 53.1 to 5.2% and the EE leveled off at ca. 52.0% in various copolymer concentrations. The results demonstrated that the maximum concentration of encapsulated rapamycin was ca. 0.5 mg/mL, regardless of polymer concentration. The LC was expected at a fixed drug concentration, therefore, quantitatively solubilized by the copolymers at the initial rapamycin concentration 1 mg/mL. In Fig. 1D, the average diameter and PDI of rapa-micelles are plotted against the copolymer concentration. At lower polymer concentrations (1.0 mg/mL), the average size of rapa-micelles was smaller but the distribution was wide, because not enough copolymers were added to saturate the rapamycin. At higher polymer concentrations (>5.0 mg/mL), the same trend was observed for average size and PDI. Copolymer concentrations of 10.0 mg/mL produced unloaded micelles averaging 98.7 nm in size, and PDIs of 0.273 [27]. The PDI results thus suggested that excess polymer probably formed unloaded micelles. Moreover, the EE was constant because the formation of empty micelles occurred at higher concentrations of copolymers.

To increase rapamycin concentration in drug carrier system, the rapa-micelles (copolymer concentration 2 mg/mL) were concentrated by membrane filtration (Sartorius VIVACON 500, 50,000 MW). After 10 min of 10,000 rpm centrifugation, a rapamycin concentration of 1.8 mg/mL was obtained, which was far higher than rapamycin's water solubility [16]. DLS analysis showed the same average size and PDI as for the initial solution, demonstrating that this method of condensation maintained particle dispersion and controlled rapamycin concentration.

3.2. Stability of rapa-micelles

Previous research demonstrated that the stability of doxorubicin-loaded micelles (Dox-micelles) depended on pH and passage of time [27]. After 24 h under physiological conditions (pH 7.4, 37 °C), the size of Dox-micelles progressively increased from 43.2 to 815.3 nm. Clear changes were observed in the average diameter of rapa-micelles, indicating significant aggregation. As shown in Fig. 2A, the average size of rapa-micelles (mixed micelles) was more stable than that of single componential micelles, but formation of rapamycin precipitates was not observed, indicating that rapamycin was stably incorporated in micelles at 37 °C and at pH 7.4. The high stability might have resulted from the hydrogen

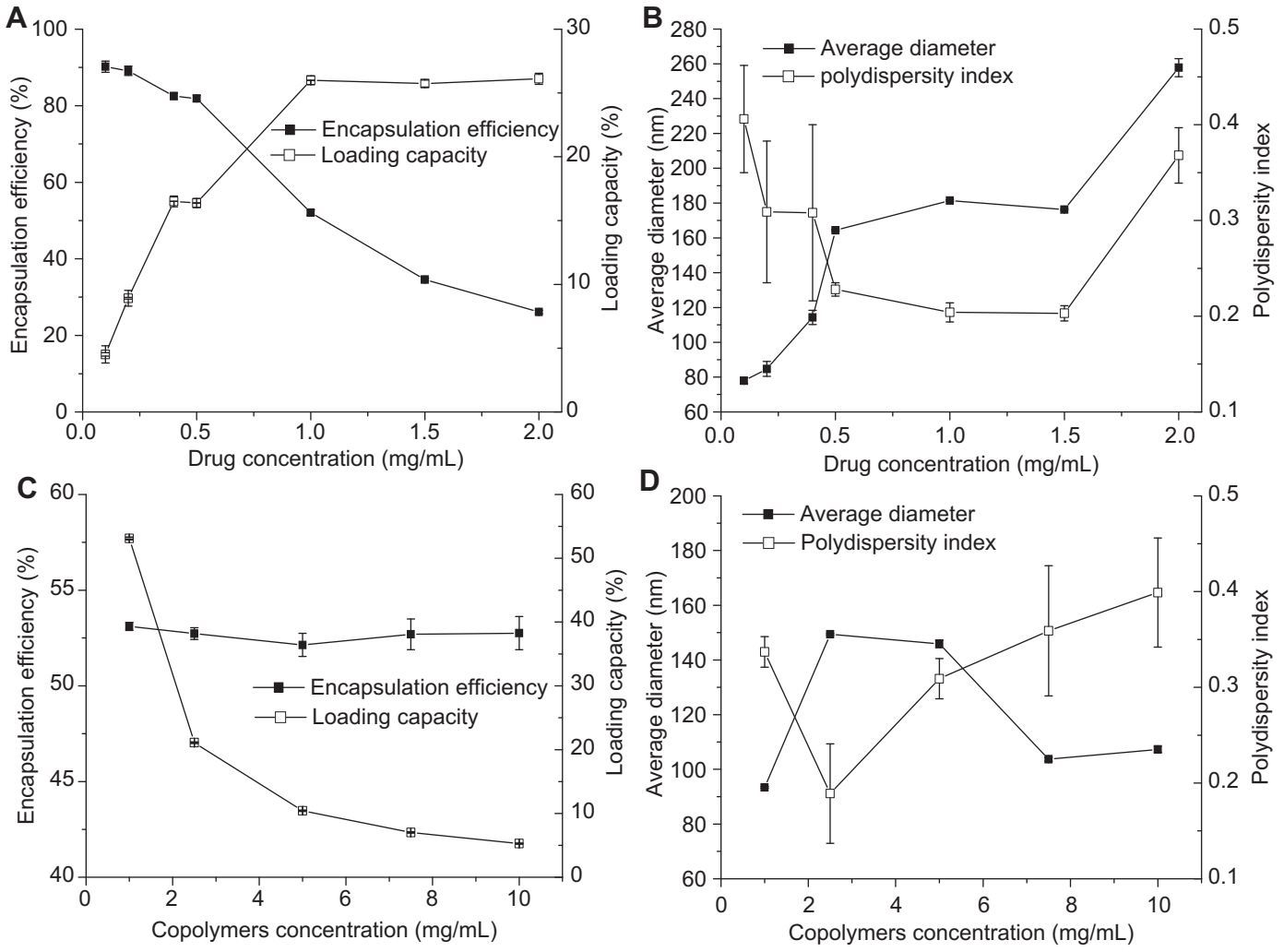

Fig. 1. The effects of rapamycin concentration on (A) encapsulation efficiency and loading capacity and (B) average diameter and polydispersity index of rapa-micelles. The effects of copolymers concentration on (C) encapsulation efficiency and loading capacity and (D) average diameter and polydispersity index of rapa-micelles. Mean ± SD ($n = 3$).

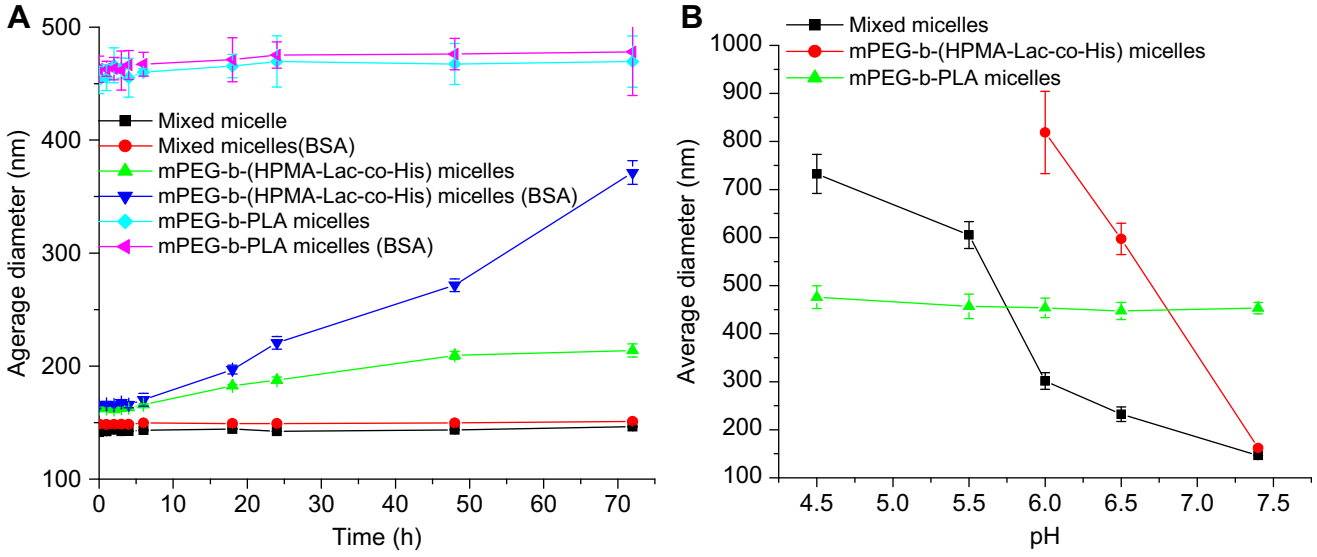

Fig. 2. (A) Evaluation of the change in micelles size in PBS buffer or PBS buffer contains 5 wt% of bovine serum albumin (BSA) at 37 °C, as determined by DLS. Mean ± SD ($n = 3$). (B) The average diameter of micelles in different pH of PBS buffers by Dynamic light scattering (DLS) analysis. mPEG-b-(HPMA-Lac-co-His) micelles disintegrated at the lower pH than 6.0. Mean ± SD ($n = 3$).

bonding and hydrophobic interactions between rapamycin and the lactate side chain of P(HPMA-Lac-*co*-His)/PLA segments [36]. In addition, mixed micelles with low-CMC copolymer prevented dissociation of any copolymer from micelles and improved the mixture's stability [37].

Previous research has evaluated certain plasma proteins using serum pharmacokinetic modeling and analyzing the efficacy data for drug-loaded micelles, to test the stability of micelles or drug-loaded micelles in the presence of serum albumins [38]. As shown in Fig. 2A, the current study found that rapamycin-loaded mixed micelles were stable in BSA solution after 72 h. Conversely, rapamycin-loaded mPEG-*b*-P(HPMA-Lac-*co*-His) micelles adsorbed BSA, because rapamycin or hydrophobic segments exposed on micelles, and interacted hydrophobically with BSA. These results indicated that low-CMC diblock copolymers helped to prevent the adsorption of albumin on micelles [37]. Mixed micelles were more stable than single componential micelles in a rapamycin delivery system because of the stronger physical interactions at the core of mixed micelles.

3.3. pH-sensitivity

This study investigated the pH and temperature sensitivity of micelles, and elucidated the application of temperature–sensitive copolymer to load rapamycin into mixed micellar structures. Rapa-micelles have been found to be highly stable after 72 h under physiological conditions. In mPEG-*b*-P(HPMA-Lac-*co*-His) diblock copolymers, the N-(2-hydroxypropyl) methacrylamide dilactate molecules not only increased the CPs, but also caused the copolymers to be prone to changes in pH associated with the protonation–deprotonation of the imidazole group of histidine. Most anti-cancer drug nanocarriers are internalized through endocytosis upon contact with the cell membrane. The triggering mechanism for these endocytosed nanomaterials must generally occur in acidic organelles to release the drug into the cytoplasm [39]. During endocytosis, pH is known to drop significantly from the physiological value (7.4–7.2) to pH 6.5–5.0 in the endosomes, and to roughly pH 5.0 in primary and secondary lysosomes. In addition, the extracellular pH of tumors (ranging from 6.8 to 6.5) is slightly more acidic than that of blood and normal tissues [40].

Empty mixed micelles displayed a pH response of less than pH 7.0 at 37 °C, and the pH-sensitive moiety (histidine) in the core–shell micelles was affected by lactic acid from the hydrophobic segment and environmental pH. Therefore, an electrostatic repulsive force apparently dissociated the empty mixed micelle structure, releasing the encapsulated drug. Fig. 2B shows the effects of pH on the average diameter of rapamycin-loaded mixed micelles and the single componential micelles in buffer solutions, as determined by DLS at 37 °C. When the pH was less than 6.5, the average diameter of mPEG-b-P(HPMA-Lac-co-His) micelles increased rapidly because the acidic environment triggered the imidazole ring and hydrolysis of lactic acid. This process caused the repulsion force of the P(HPMA-Lac-*co*-His) segments to dissociate the micellar structure. Conversely, the particle size of rapamycin-loaded mixed micelles slightly increased in the pH range 7.4 to 6.0, and below pH 6.0 the average diameter increased sharply, indicating that mPEG-b-PLA copolymer restricted the mPEG-b-P(HPMA-Lac-co-His) copolymer to reduce the mobility and repulsion force of histidine.

Morphological analysis by TEM was also applied to identify the structural dissociation of rapa-micelles under different pH conditions. Fig. 3 shows the core–shell structure of rapamycin-loaded mixed micelles under three different pH conditions, observed using 2% uranyl acetate as the contrast agent. At pH 7.4, the dark region of the hydrophobic segments and rapamycin represent the inner core, and hydrophilic segments of mPEG extend outside the core. In acidic media, micellar cores were protonized and we observed structural dissociation, irregular multilayering (Fig. 4B, arrowhead), and drug aggregation to form fragments. The acidic buffer solution was diffused into the inner core to change the structure. These results illustrated the pH-sensitivity and core–shell structure of the rapa-micelles.

3.4. pH-dependent drug release

Because the structure of rapamycin has no ionizable functional grouping, pH adjustment does not affect its aqueous solubility [16]. As mentioned above, rapa-micelles were pH-responsive and encapsulated rapamycin stably. A relatively high temperature (37 °C) was found to facilitate the release of the drug from micelles because the hydrolysis rate of lactic acid side groups increased at higher temperatures [41]. To verify the effectiveness of rapa-micelles for intracellular drug delivery, we compared the performance of micelles under physiological conditions (pH 7.4) versus an endosomal (pH 6.5) or lysosomal (pH 5.0) environment. Fig. 4A plots the drug release profile of rapa-micelles at 37 °C. At pH 7.4, no significant release of rapamycin from the micelles was initially observed. The encapsulated rapamycin reduced the initial drug release burst because of the relatively strong physical interactions between copolymer and drug. However, at a pH of 6.5 or 5.0, much of the drug was released within 5 h, namely 35.2% and 57.6%, respectively. Under acidic conditions, the imidazole group protonation and hydrolysis of lactic acid side groups deformed the micellar structure, releasing rapamycin from the mixed micelles. The pH-sensitive release profile corroborated the claim that micelles are pH sensitive, because changes in pH deformed their core structure and released the rapamycin. The rapamycin release profile of mixed micelles at 25 °C was shown in Fig. 4B, pHs of 5.4,

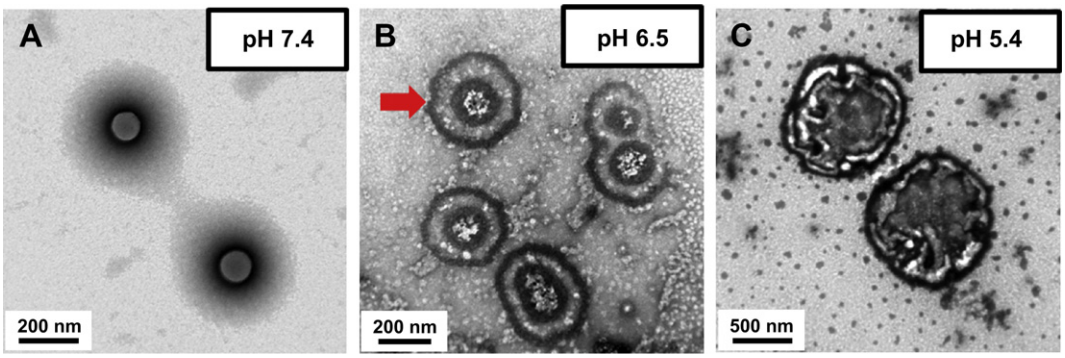

Fig. 3. Transmission electron microscopy (TEM) images of rapa-micelles in PBS buffer at pH (A) 7.4, (B) 6.5 and (C) 5.4 for 1 h.

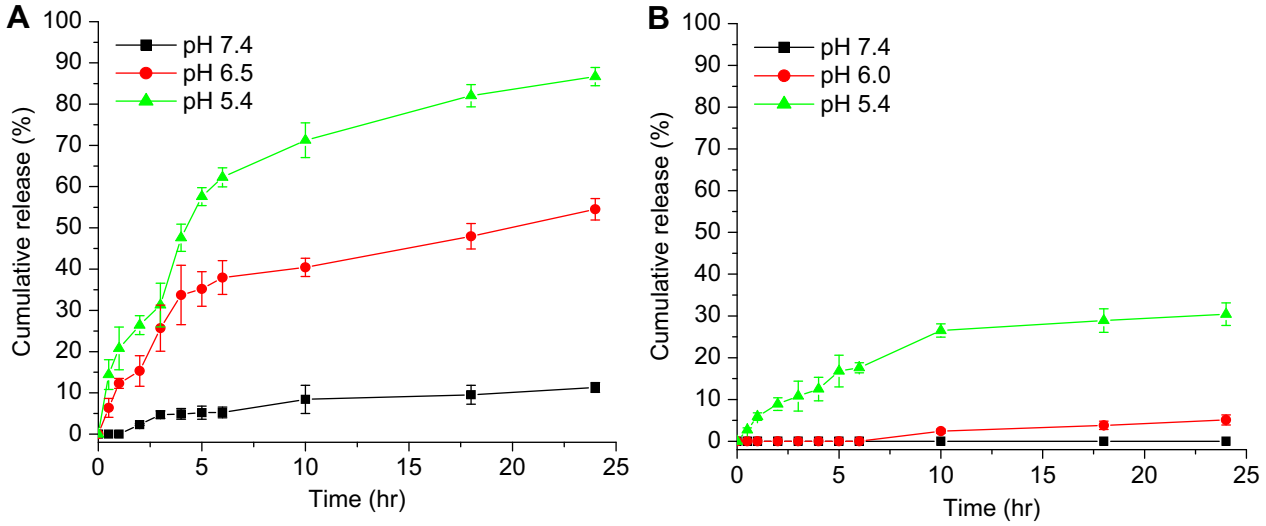

Fig. 4. Effect of pH on rapamycin release from mixed micelle *in vitro* at 37 °C (A) and 25 °C (B). Mean ± SD ($n = 3$).

6.5 and 7.4, 0, 0 and 12.5% of the drug was released within 5 h, respectively. Fig. 4B demonstrated the high stability of rapamycin-loaded micelles and no burst release in the neutral and slight acidic (pH 6.5) environment at 25 °C. At either temperature, release speed at pH 5.4 was higher than at pH 7.4. From comparison of Fig. 4A and B, a higher temperature was found to be helpful for drug release because the hydrolysis rate of lactic acid side groups increased at higher temperature [37], which makes hydrophobic drug movement within the hydrophobic core easier. Notably, the release behavior of mixed micelles in room temperature could help to store rapamycin and be less pH-dependent.

3.5. Intracellular localization of micelles

The current study used CLSM to monitor the HCT116, which were incubated with Cy5.5-tagged rapa-micelles at 37 °C for 1 and 6 h, and thereafter showed a spotted red fluorescence pattern (Fig. 5). Colocalization of the micelles with cell nuclei (DAPI, blue fluorescence) and endo-lysosome (lysotracter, green fluorescence) revealed that micelles were internalized closed to nuclei and observed in the cytoplasm, wherein the LysoTracker molecules were also located indicating that the mixed micelles were taken up from extracellular fluid into cells by endocytosis. The triggering mechanisms occur in the acidic intracellular endo-lysosomal compartment after endocytosis. After 6 h, Cy5.5-tagged rapa-micelles more obvious with increasing time also localized in endo-lysosome. Fig. 5 has demonstrated that PEG modified micelles were trapped in the endocytic vesicles because PEG modified particles with caveolae are absorbed efficiently through a number of routes [28]. Caveolae illustrate the major non-clathrin dependent route from the cell surface to endosomes [29]. This result was similar to our previous studies [27,42,43]. Moreover, released rapamycin could use to induce autophagolysosome and help to increase the fluorescence intensity of lysosomal marker

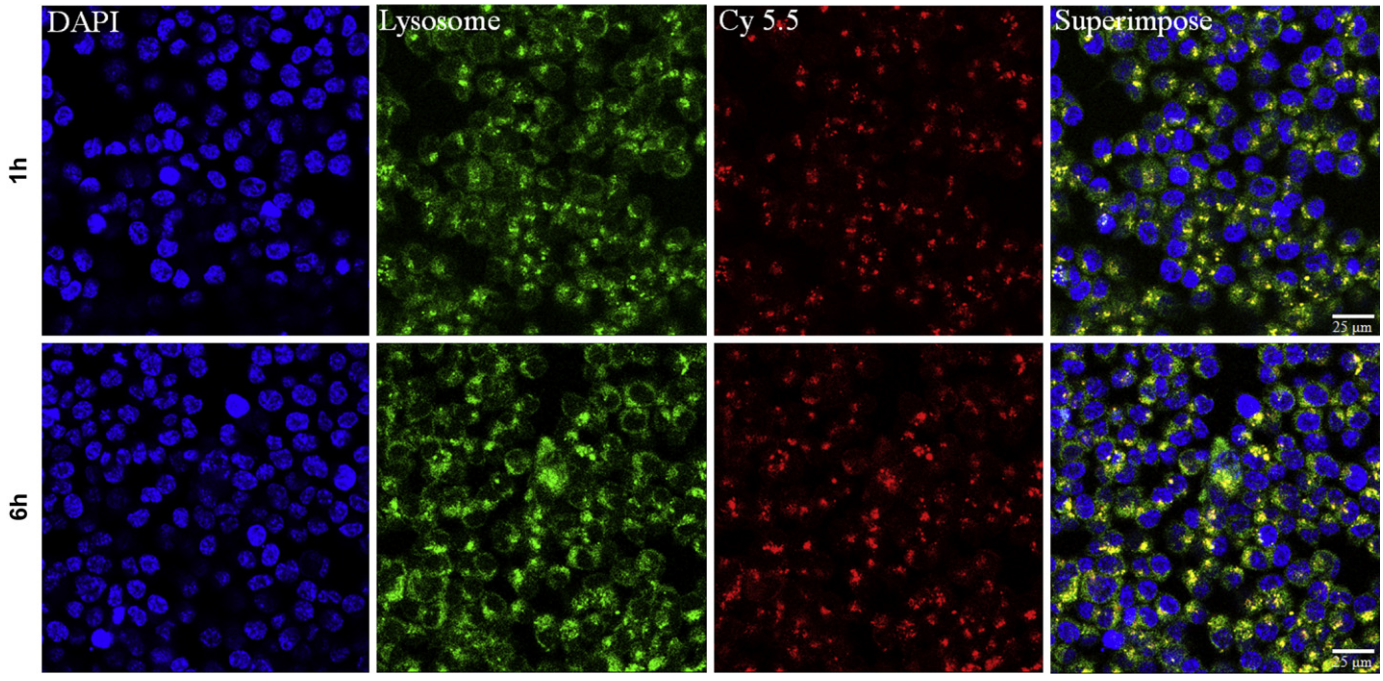

Fig. 5. Confocal images of HCT116 incubated with Cy5.5as tagged rapa-micelle and at 37 °C.

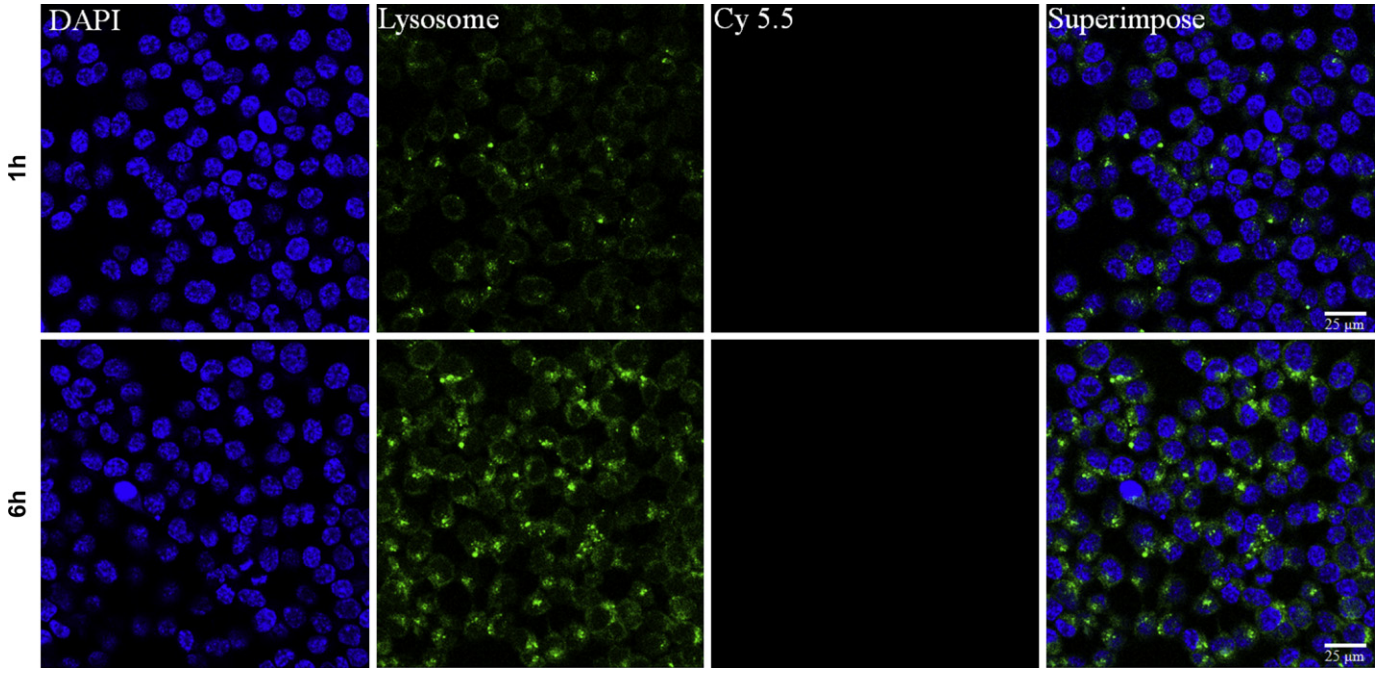

Fig. 6. Confocal images of HCT116 incubated with rapamycin and at 37 °C after 1 and 6 h.

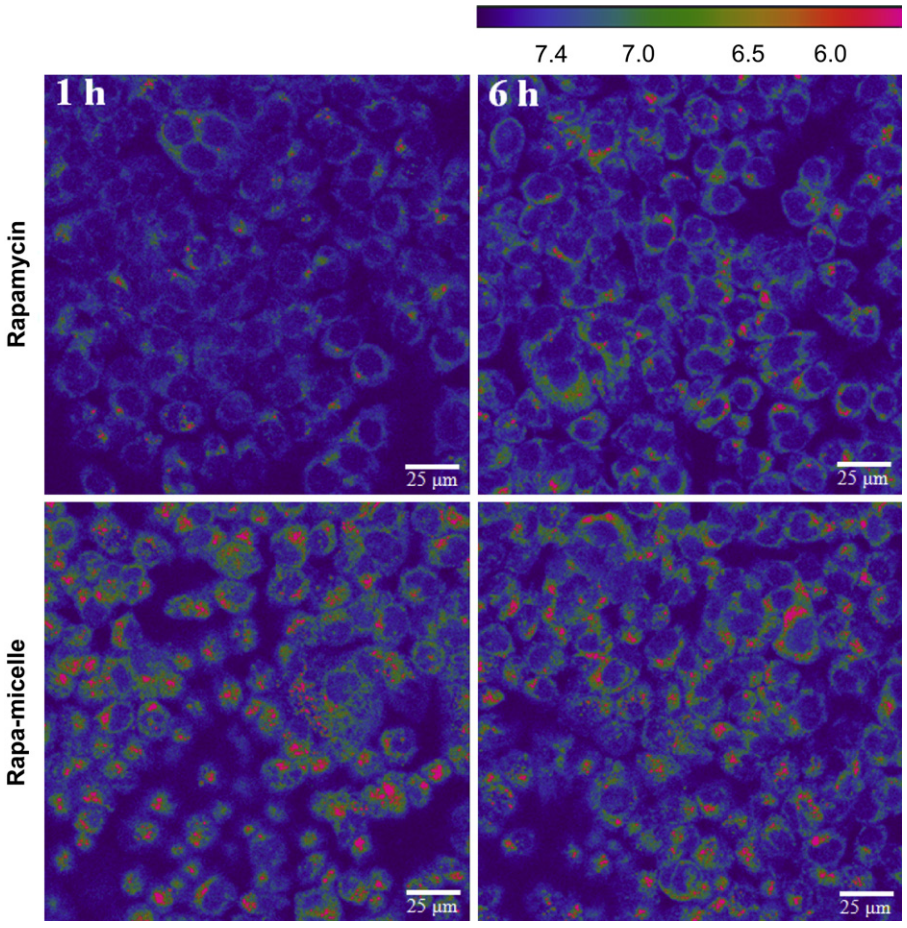

Fig. 7. False-color ratiometric imaging of pH of HCT116 cells incubated with rapamycin and rapa-micelle at 37 °C after 1 and 6 h.

LysoTracker. On the other hand, HCT116 cells incubated with free rapamycin for 1 h showed the weak fluorescence intensity of lysosomal marker LysoTracker (Fig. 6). After 6 h, free rapamycin more obvious with increasing time also increased the fluorescence intensity of lysosomal marker. The result ascribed that free rapamycin was passive diffusion into HCT116 cells and induced autophagosomes than fuse with lysosomes.

The pH monitoring technique offers an advantage over currently available natural and synthetic fluorescent probe molecules. Fluorescent indicators that exhibit pH-driven wavelength alterations in their emission spectra allow for reliable detection of, for example, SNARF-1-AM and 2,7-bis(2-Carboxyethyl)-5(6)-carboxyfluorescein acetoxymethyl ester [44]. SNARF-1 enters cells in the diacetate form (SNARF-1-AM), and is then hydrolyzed by cellular esterase and trapped as SNARF-1. SNARF-1 is a single-excitation dual-emission fluorescent probe and its optical properties make it appropriate for ratiometric imaging by CLSM, so that intracellular pH changes can be quantitatively measured [45]. To clarify the intracellular pH precisely and promptly, pH topography was determined by loading cells with the ratiometric fluorescent probe SNARF-1. The HCT116 cells incubated with rapamycin and rapa-micelles at 37 °C showed false-color ratiometric imaging (Fig. 7). After 1 h, ratiometric imaging of the HCT116 cells incubated with rapa-micelles showed the low pH of the lysosomal compartment could be exploited by generating acid-labile rapa-micelles that would be activated in the lysosomal compartment. Following rapa-micelle uptake, the particles were monitored and found to reside in intracellular compartments with pH values below 6.5. Rapa-micelles are disintegrated through structural changes below pH 6.5, the hydrophobic drug can be released into cell effectively and in an initially more controlled manner in acidic endocytic compartments (Scheme 1). Moreover, released rapamycin induced autophagosomes then fuse with lysosomes, containing acid hydrolases. After 6 h, ratiometric imaging of the HCT116 cells incubated with rapa-micelles also showed the low pH range. Conversely, the pH of HCT116 cells incubated with free rapamycin did not decrease significantly after 1 h. This results also demonstrated that the drug merely diffused passively into the cells, therefore, the cells did not occurs through endocytosis. After 6 h, ratiometric imaging of the HCT116 cells incubated with rapamycin showed the low pH range because of the autophagolysosome. Therefore, this observation complied with the expected pattern and demonstrated the pH values ranging after internalization of the micelles by endocytosis, through which the micelles end up in the acidic environment.

3.6. Immunofluorescence assay

The induction of autophagy was evaluated by detecting an increase of the autophagosomal membrane form of microtubule-associated protein 1 light chain 3 (LC3). Microscopic analysis of the formation of LC3 punctate structures is widely used to monitor autophagosome formation. Immunofluorescence analysis employing the anti-human microtubule-associatedprotein 1 light chain 3 isoform B (anti-LC3B) antibody has been shown to be useful in monitoring autophagy in HCT116 cell line, which were incubated with rapa-micelles and rapamycin at 37 °C for 1 and 6 h (Fig. 8). After 1 and 6 h, rapa-micelles can induce more accumulation of LC3-positive punctuate than rapamycin. Several reasons may explain rapa-micelles enhance autophagy. We suggest rapa-

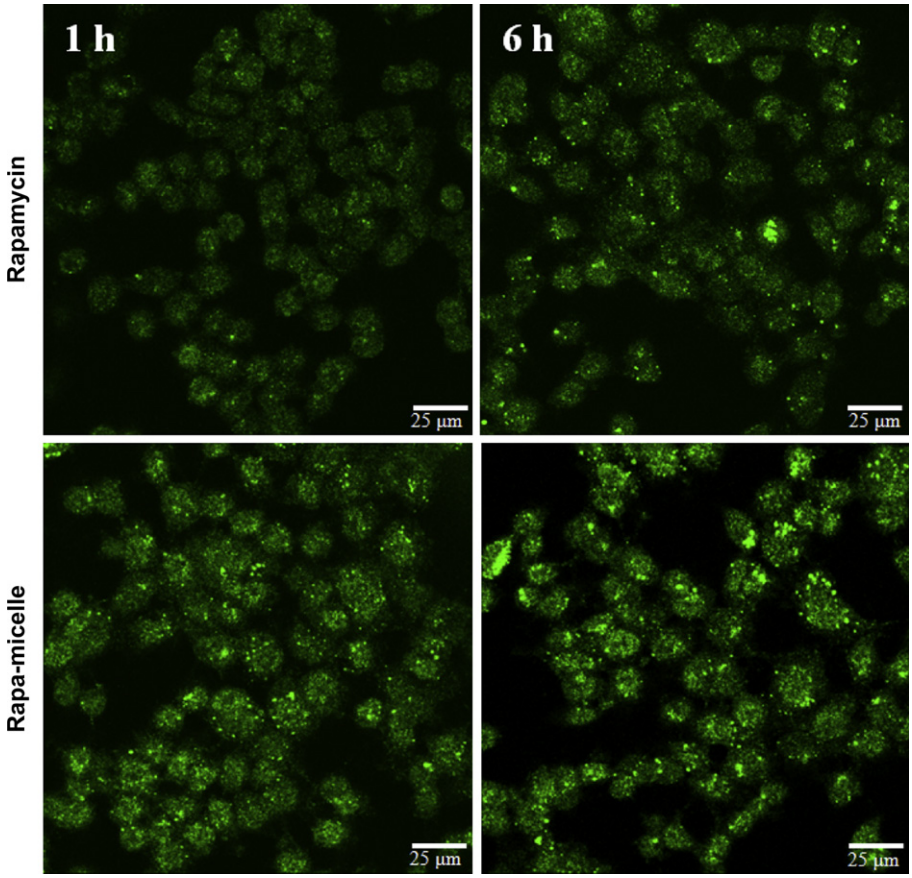

Fig. 8. LC3 immunofluorescence of HCT116 cells incubated with rapamycin and rapa-micelle at 37 °C after 1 and 6 h.

micelles entered the cells via endocytosis pathway, nanoparticle induced the adaptive cellular response [46] and/or released rapamycin induced autophagy.

3.7. Cytotoxicity

For the *in vitro* experiments, micellar integrity was determined from the final copolymer concentration of 1.6 mg/mL, which is much higher than CMC. To compare cytotoxic activity of the loaded versus free drug, HCT116 and HeLa cells were exposed to a series of equivalent concentrations of free rapamycin or rapamycin encapsulated in micelles for 24 and 72 h. The percentage of viable cells was quantified using a tetrazolium dye (MTS) assay. As a negative control, empty micelles were added to equivalent concentrations as that of prepared rapa-micelles (i.e. the same concentration of mixed micelle-forming material). Empty micelles displayed no significant cytotoxicity, either towards the two cancer cell lines or towards the normal human foreskin fibroblast HS68 cell, as tested after 24 or 72 h *in vitro*. These results indicated that the empty micelles were not cytotoxic (Fig. 9A). In contrast, the viability of the two cancer cell lines was strongly influenced by rapamycin concentration (Fig. 9B and C).

Table 1
IC50 values of rapamycin and rapa-micelles in cancer cells after 24 h and 72 h drug exposure.

Cell lines	IC_{50} (μg/mL)			
	Rapamycin		Rapa-micelle	
	24 h	72 h	24 h	72 h
HCT116	10.22	2.40	7.81	0.70
HeLa	118.57	20.44	95.39	9.23

Table 1 shows the inhibition concentration (IC_{50}) of free drug and rapa-micelles. Both the free drug and the rapa-micelles were more cytotoxic at lower concentrations after 72 h of incubation compared with 24 h. Notably, comparisons of the cytotoxic potency of rapa-micelles versus free drug showed that rapa-micelles exhibited a considerably superior cytotoxic potency against HCT661 and HeLa cells. We concluded that the enhanced uptake of rapa-micelles occurred because of their assisted clathrin-dependent endocytosis, relative to the passive diffusion of rapamycin through the cell membrane in the free drug condition. The increased uptake of micelles occurred by a fluid-phase endocytosis

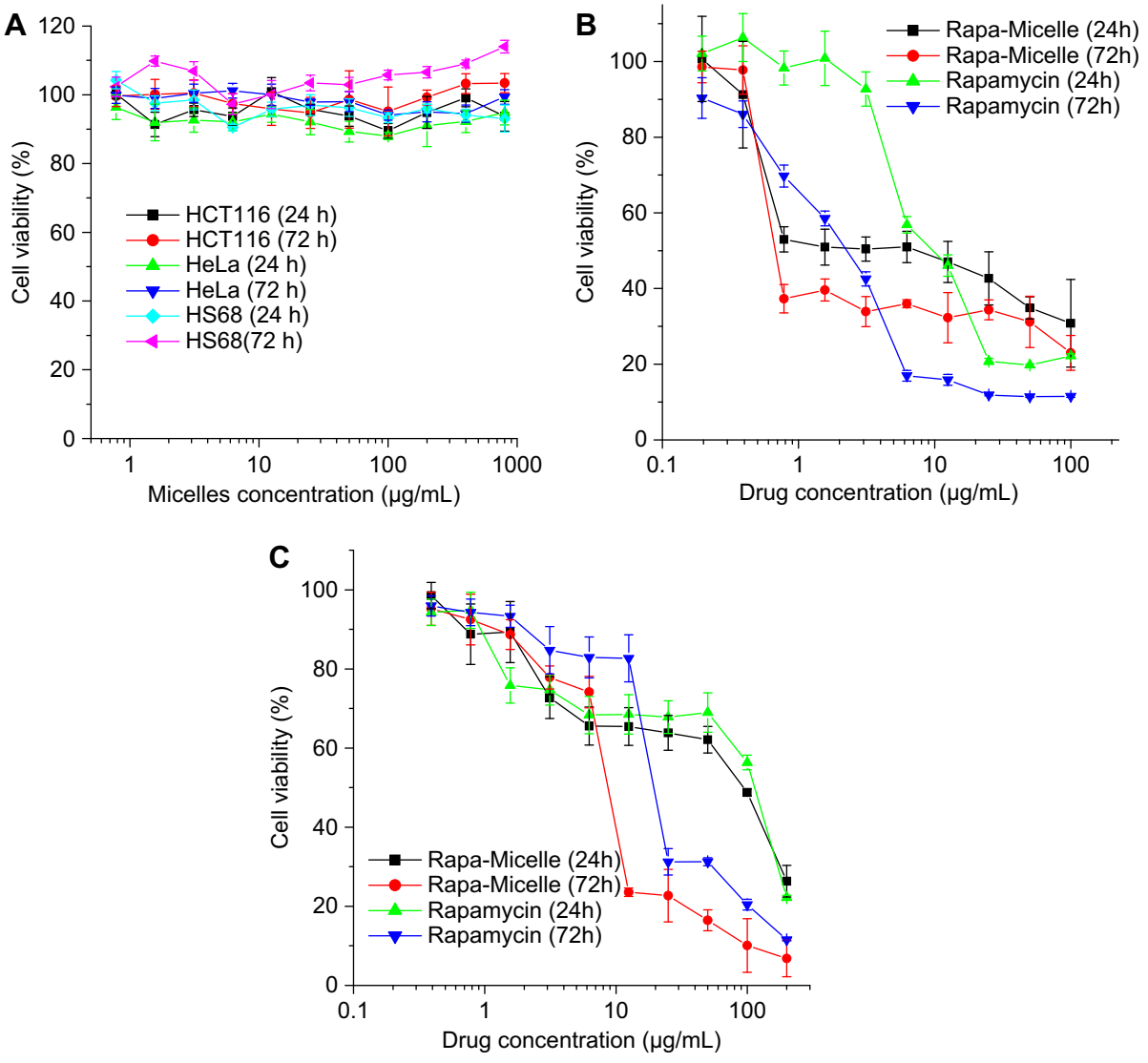

Fig. 9. Cytotoxicity of (A) empty micelle, rapamycin and rapa-micelles on HCT116 (B), HeLa (C) and HS-68 cells after 24 and 72 h of incubation *in vitro*. Data are the means and standard deviations of eight independent experiments.

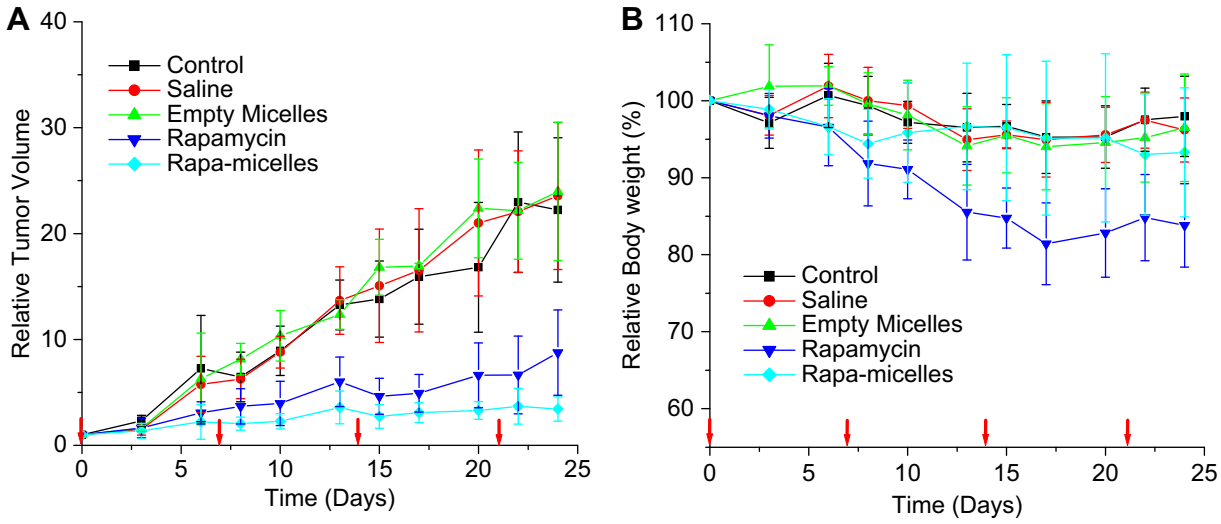

Fig. 10. (A) *In vivo* anticancer efficacy and (B) body weight changes in Balb-c/nude mice bearing HCT-116 tumors after intravenous administration of controlled, empty micelle, saline, free rapamycin and rapa-micelles. Mice were treated intravenous *via* the tail vein at 4 different time points with an interval of 7 days.

mechanism because no specific affinity existed between the outer PEG chains of the micelles and negatively charged plasma membrane of the cells [47,48]. The results indicated that the use of polymeric micelles enhances cytotoxic efficiency in a similar manner to that of other particulate [47], and which we had previously also reported [27].

3.8. *In vivo* antitumor activity

The delivery of drugs with poor water-solubility remains a crucial problem in the clinical development of anticancer therapy. A recent study found that 75% of candidates for drug development have low solubility [49]. Various conventional excipients have been

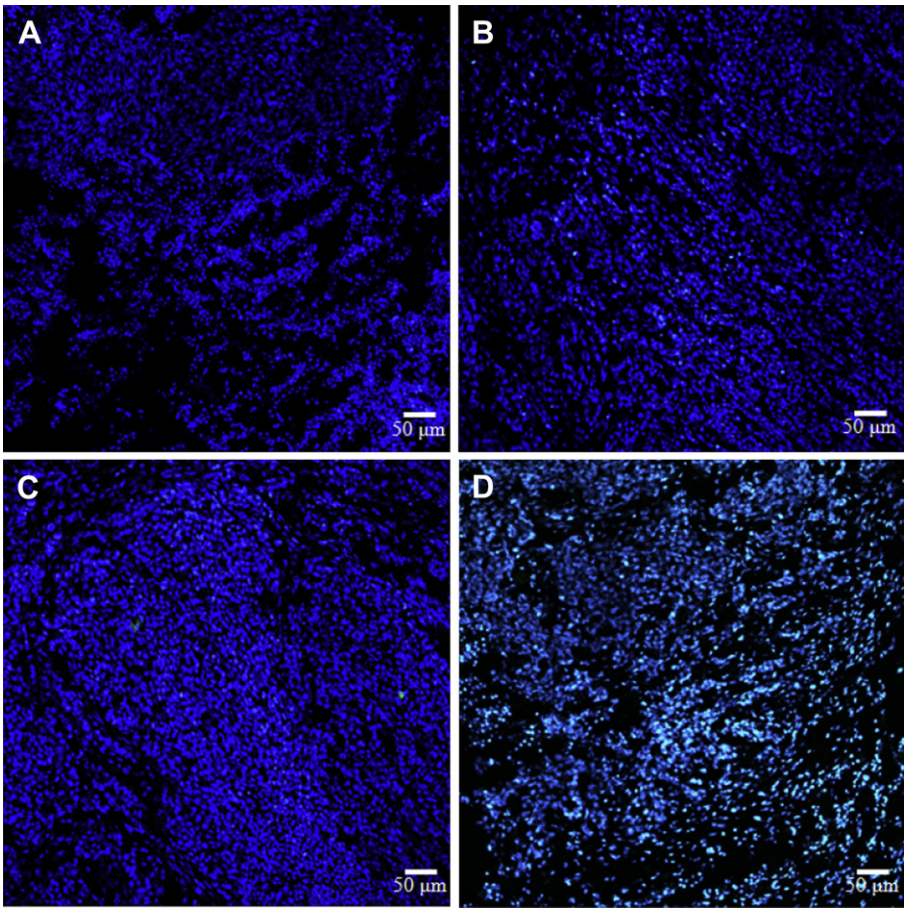

Fig. 11. TUNEL apoptotic cell detection of tumor cell in tumor-bearing mice after intravenous administration of (A) saline (B) empty micelles (C) free rapamycin and (D) rapa-micelles. Green: apoptotic cells; blue: DAPI. (For interpretation of the references to colour in this figure legend, the reader is referred to the web version of this article.)

designated as Class II (low solubility and high permeability) compounds in the Biopharmaceutics *Classification* System (BCS), rendering aqueous solubility the limiting factor regarding bioavailability [50]. Common techniques to improve drug solubility include the use of co-solvents or surface-active agents. Many formulation production processes used for poorly water-soluble drugs, such as spray drying, rotary evaporation, precipitation methods, and freeze-drying methods, require the use of solvents; these solvents may be organic or inorganic and many are highly toxic. Thus they must be present only at extremely low levels in the final product, if at all, to reduce the risk to the patient [51]. Moreover, certain ingredients in traditional excipients that are used to disperse the substrate (eg. Cremophor EL and Tween 80) run the risk of precipitation and incidental adverse effects, including acute hypersensitivity reactions, edema, and peripheral neuropathy [52,53].

To examine *in vivo* antitumor efficacy of rapa-micelles, Balb-c/nude mice bearing human colon tumor were treated with saline, empty micelles, rapamycin or rapa-micelles. All the treatment modalities were administered by intravenous injection with a frequency of four times at a 7 day interval when the tumors reached a volume of 50 mm^3. The growth of subcutaneously-implanted tumors was assessed over a 24-day time frame. Tumor volumes of the untreated (control) increased very rapidly (ca. 22.2-fold increase) (Fig. 10A). In addition, tumor volumes of the empty micelles and saline showed the same trend as control. Empty micelles displayed no antitumor activity and were non-effect on the treatment. Mice treated with free rapamycin and rapa-micelles showed slow increase (8.8- and 3.4-fold, respectively) after 24 days. Clearly the results suggest that rapa-micelles showed a considerably higher antitumor activity compared with free rapamycin. The traditional formation of rapamycin is associated with some acute side effects. Body weight loss is one of indicators to evaluate free drug- and excipients-induced toxicity. Mice treated with free rapamycin in 4% ethanol/5% PEG 400/5% Tween 80 aqueous solution exhibited a 15% decrease of body weight within 22 days (4 injections), and appeared to be weak after treatment (Fig. 10B). Treatment with rapa-micelles resulted in a minimal weight loss (approximately 5%), suggesting that this drug carrier could phenomenal reduce rapamycin and excipients-induced toxicity to normal tissues. Untreated and treated with saline and empty micelles showed the mice kept weight because the tumor volumes increased rapidly. Therefore, the therapeutic efficiency could be maximized while minimizing unwanted side effects from excipients such as toxicity. This better *in vivo* antitumor activity suggests that rapa-micelles incorporated with the selective targeting, tumor-specific accumulation and effective release in the both endocytosis and autophagy pathway.

3.9. Tumor apoptosis

Evidence suggests that rapamycin could induce G1–S cell cycle arrest and eventually apoptosis depending on cellular characteristics of tumor cells [54–56]. Tumor apoptosis (from biopsy specimens obtained from the middle of the lesion) revealed by TUNEL staining [26] after 22 days of treatment with saline, empty micelles, rapamycin or rapa-micelles (Fig. 11). In addition, DAPI was used to stain nuclei of tumor cells. Results showed that both controlled treatment and free rapamycin did not induce significant apoptosis of tumor cells above the control level. On the other hand, rapa-micelles induced higher rates of apoptosis in tumor cells as measured by TUNEL assay. These confocal images clearly indicate that rapa-micelles provide a higher therapeutic efficacy compared with the free rapamycin.

4. Conclusions

In this study, we demonstrated that our previously described performance enabled temperature- and pH-sensitive micelles to efficiently encapsulate the hydrophobic drug rapamycin. Our heat shock protocol did not require toxic co-solvents or harsh surfactants to stabilize the hydrophobic drug. The encapsulated rapamycin showed excellent size stability in the presence of aqueous and BSA serum media. All materials used in this study were relatively safe and were highly sensitive to intracellular pH changes. The uptake studies indicated that micelles delivered the drug efficiently to the cells through endocytosis. The size and structure of micelles could enhance the delivery of the drug to a tumor through the EPR effect and the release of the drug into the extracellular tumor microenvironment. Moreover, the carrier is non-cytotoxic and enhanced the cytotoxicity of the rapamycin *in vitro* and *in vivo*. All these features point to a system that is a promising candidate in the clinical treatment of rapamycin-sensitive tumors.

Acknowledgments

This work was supported partly by Department of Health of the Republic of China, Taiwan for financially supporting this work with National Research Program for Biopharmaceuticals (DOH101-TD-PB-111-TM011/101TM007) and partly by another grant from the National Science Council of the Republic of China (100/101-2120-M-033-001- and 101-2221-E-033-035-). Prof. Tian-Lu Cheng and Dr. Chien-Han Kao (Department of Biomedical Science and Environmental Biology, Kaohsiung Medical University, Kaohsiung, Taiwan) are appreciated for kindly providing the comments for this research. We thank the excellent technical assistance of Technology Commons, College of Life Science, NTU (Taiwan) with CLSM and TEM.

Appendix A. Supplementary data

Supplementary data related to this article can be found at http://dx.doi.org/10.1016/j.biomaterials.2012.10.034.

References

[1] Vezina C, Kudelski A, Sehgal SN. Rapamycin (AY-22,989), a new antifungal antibiotic. I. Taxonomy of the producing streptomycete and isolation of the active principle. J Antibiot (Tokyo) 1975;28:721–6.
[2] Abraham RT, Wiederrecht GJ. Immunopharmacology of rapamycin 1. Annu Rev Immunol 1996;14:483–510.
[3] Sabatini DM. mTOR and cancer: insights into a complex relationship. Nat Rev Cancer 2006;6:729–34.
[4] Marinov M, Fischer B, Arcaro A. Targeting mTOR signaling in lung cancer. Crit Rev Oncol Hematol 2007;63:172–82.
[5] Ji J, Zheng P-S. Activation of mTOR signaling pathway contributes to survival of cervical cancer cells. Gynecol Oncol 2010;117:103–8.
[6] Gulhati P, Cai Q, Li J, Liu J, Rychahou PG, Qiu S, et al. Targeted inhibition of mammalian target of rapamycin signaling inhibits tumorigenesis of colorectal cancer. Clin Cancer Res 2009;15:7207–16.
[7] Noh W-C, Mondesire WH, Peng J, Jian W, Zhang H, Dong J, et al. Determinants of rapamycin sensitivity in breast cancer cells. Clin Cancer Res 2004;10:1013–23.
[8] Kroemer G, Jaattela M. Lysosomes and autophagy in cell death control. Nat Rev Cancer 2005;5:886–97.
[9] Mizushima N, Levine B, Cuervo AM, Klionsky DJ. Autophagy fights disease through cellular self-digestion. Nature 2008;451:1069–75.
[10] Faivre S, Kroemer G, Raymond E. Current development of mTOR inhibitors as anticancer agents. Nat Rev Drug Discov 2006;5:671–88.
[11] Wanner K, Hipp S, Oelsner M, Ringshausen I, Bogner C, Peschel C, et al. Mammalian target of rapamycin inhibition induces cell cycle arrest in diffuse large B cell lymphoma (DLBCL) cells and sensitises DLBCL cells to rituximab. Br J Haematol 2006;134:475–84.
[12] Raught B, Gingras A-C, Sonenberg N. The target of rapamycin (TOR) proteins. Proc Natl Acad Sci U S A 2001;98:7037–44.
[13] Buck E, Eyzaguirre A, Brown E, Petti F, McCormack S, Haley JD, et al. Rapamycin synergizes with the epidermal growth factor receptor inhibitor

erlotinib in non–small-cell lung, pancreatic, colon, and breast tumors. Mol Cancer Ther 2006;5:2676–84.
[14] Guba M, Koehl GE, Neppl E, Doenecke A, Steinbauer M, Schlitt HJ, et al. Dosing of rapamycin is critical to achieve an optimal antiangiogenic effect against cancer. Transpl Int 2005;18:89–94.
[15] Seeliger H, Guba M, Kleespies A, Jauch K-W, Bruns C. Role of mTOR in solid tumor systems: a therapeutical target against primary tumor growth, metastases, and angiogenesis. Cancer Metastasis Rev 2007;26:611–21.
[16] Simamora P, Alvarez JM, Yalkowsky SH. Solubilization of rapamycin. Int J Pharm 2001;213:25–9.
[17] Napoli KL, Wang M-E, Stepkowski SM, Kahan BD. Distribution of sirolimus in rat tissue. Clin Biochem 1997;30:135–42.
[18] Chen M-C, Tsai H-W, Liu C-T, Peng S-F, Lai W-Y, Chen S-J, et al. A nanoscale drug-entrapment strategy for hydrogel-based systems for the delivery of poorly soluble drugs. Biomaterials 2009;30:2102–11.
[19] Yuan X-B, Yuan Y-B, Jiang W, Liu J, Tian E-J, Shun H-M, et al. Preparation of rapamycin-loaded chitosan/PLA nanoparticles for immunosuppression in corneal transplantation. Int J Pharm 2008;349:241–8.
[20] Forrest ML, Won C-Y, Malick AW, Kwon GS. In vitro release of the mTOR inhibitor rapamycin from poly(ethylene glycol)-b-poly([epsilon]-caprolactone) micelles. J Control Release 2006;110:370–7.
[21] Lu W, Li F, Mahato RI. Poly(ethylene glycol)-block-poly(2-methyl-2-benzoxycarbonyl-propylene carbonate) micelles for rapamycin delivery: in vitro characterization and biodistribution. J Pharm Sci 2011;100:2418–29.
[22] Bisht S, Feldmann G, Koorstra J-BM, Mullendore M, Alvarez H, Karikari C, et al. In vivo characterization of a polymeric nanoparticle platform with potential oral drug delivery capabilities. Mol Cancer Ther 2008;7:3878–88.
[23] Parhi P, Mohanty C, Sahoo SK. Enhanced cellular uptake and in vivo pharmacokinetics of rapamycin-loaded cubic phase nanoparticles for cancer therapy. Acta Biomater 2011;7:3656–69.
[24] Maeda H. Tumor-selective delivery of macromolecular drugs via the EPR Effect: background and future prospects. Bioconjug Chem 2010;21:797–802.
[25] Stefanadis C, Chrysochoou C, Markou D, Petraki K, Panagiotakos DB, Fasoulakis C, et al. Increased temperature of malignant urinary bladder tumors in vivo: the application of a new method based on a catheter technique. J Clin Oncol 2001;19:676–81.
[26] Lee ES, Gao Z, Bae YH. Recent progress in tumor pH targeting nanotechnology. J Control Release 2008;132:164–70.
[27] Chen Y-C, Liao L-C, Lu P-L, Lo C-L, Tsai H-C, Huang C-Y, et al. The accumulation of dual pH and temperature responsive micelles in tumors. Biomaterials 2012; 33:4576–88.
[28] Nativo P, Prior IA, Brust M. Uptake and intracellular fate of surface-modified gold nanoparticles. ACS Nano 2008;2:1639–44.
[29] Pelkmans L, Bürli T, Zerial M, Helenius A. Caveolin-stabilized membrane domains as multifunctional transport and sorting devices in endocytic membrane traffic. Cell 2004;118:767–80.
[30] Venn AA, Tambutté E, Lotto S, Zoccola D, Allemand D, Tambutté S. Imaging intracellular pH in a reef coral and symbiotic anemone. Proc Natl Acad Sci U S A 2009;106:16574–9.
[31] Färber K, Schumann B, Miersch O, Roos W. Selective desensitization of jasmonate- and pH-dependent signaling in the induction of benzophenanthridine biosynthesis in cells of *Eschscholzia californica*. Phytochemistry 2003; 62:491–500.
[32] Kim JH, Johannes L, Goud B, Antony C, Lingwood CA, Daneman R, et al. Noninvasive measurement of the pH of the endoplasmic reticulum at rest and during calcium release. Proc Natl Acad Sci U S A 1998;95:2997–3002.
[33] Kisiday J, Jin M, Kurz B, Hung H, Semino C, Zhang S, et al. Self-assembling peptide hydrogel fosters chondrocyte extracellular matrix production and cell division: implications for cartilage tissue repair. Proc Natl Acad Sci U S A 2002; 99:9996–10001.
[34] Gref R, Domb A, Quellec P, Blunk T, Müller RH, Verbavatz JM, et al. The controlled intravenous delivery of drugs using PEG-coated sterically stabilized nanospheres. Adv Drug Deliv Rev 1995;16:215–33.
[35] Pichon C, Gonçalves C, Midoux P. Histidine-rich peptides and polymers for nucleic acids delivery. Adv Drug Deliv Rev 2001;53:75–94.
[36] Soga O, van Nostrum CF, Fens M, Rijcken CJF, Schiffelers RM, Storm G, et al. Thermosensitive and biodegradable polymeric micelles for paclitaxel delivery. J Control Release 2005;103:341–53.
[37] Lo C-L, Lin S-J, Tsai H-C, Chan W-H, Tsai C-H, Cheng C-HD, et al. Mixed micelle systems formed from critical micelle concentration and temperature-sensitive diblock copolymers for doxorubicin delivery. Biomaterials 2009;30:3961–70.
[38] Park J, Kurosawa S, Watanabe J, Ishihara K. Evaluation of 2-Methacryloyloxyethyl phosphorylcholine polymeric nanoparticle for immunoassay of C-reactive protein detection. Anal Chem 2004;76:2649–55.
[39] Hubbell JA. Enhancing drug function. Science 2003;300:595–6.
[40] Tannock IF, Rotin D. Acid pH in tumors and its potential for therapeutic exploitation. Cancer Res 1989;49:4373–84.
[41] Coffin M, McGinity J. Biodegradable pseudolatexes: the chemical stability of poly(d, l-lactide) and poly (ε-caprolactone) nanoparticles in aqueous media. Pharm Res 1992;9:200–5.
[42] Lo C-L, Huang C-K, Lin K-M, Hsiue G-H. Mixed micelles formed from graft and diblock copolymers for application in intracellular drug delivery. Biomaterials 2007;28:1225–35.
[43] Tsai H-C, Chang W-H, Lo C-L, Tsai C-H, Chang C-H, Ou T-W, et al. Graft and diblock copolymer multifunctional micelles for cancer chemotherapy and imaging. Biomaterials 2010;31:2293–301.
[44] Weiner ID, Hamm LL. Use of fluorescent dye BCECF to measure intracellular pH in cortical collecting tubule. Am J Physiol Renal Physiol 1989;256:957–64.
[45] Buckler KJ, Vaughan-Jones RD. Application of a new pH-sensitive fluoroprobe (carboxy-SNARF-1) for intracellular pH measurement in small, isolated cells. Pflugers Arch 1990;417:234–9.
[46] Halamoda Kenzaoui B, Chapuis Bernasconi C, Guney-Ayra S, Juillerat-Jeanneret L. Induction of oxidative stress, lysosome activation and autophagy by nanoparticles in human brain-derived endothelial cells. Biochem J 2012; 441:813–21.
[47] Yoo HS, Park TG. Biodegradable polymeric micelles composed of doxorubicin conjugated PLGA–PEG block copolymer. J Control Release 2001;70:63–70.
[48] Zhang Y, Kohler N, Zhang M. Surface modification of superparamagnetic magnetite nanoparticles and their intracellular uptake. Biomaterials 2002;23: 1553–61.
[49] Di L, Kerns EH, Carter GT. Drug-like property concepts in pharmaceutical design. Curr Pharm Des 2009;15:2184–94.
[50] O'Donnell KP, Williams RO. In: Williams Iii ROO, Watts ABB, Miller DAA, editors. Optimizing the formulation of poorly water-soluble drugs formulating poorly water soluble drugs. New York: Springer; 2012. p. 27–93.
[51] Witschi C, Doelker E. Residual solvents in pharmaceutical products: acceptable limits, influences on physicochemical properties, analytical methods and documented values. Eur J Pharm Biopharm 1997;43:215–42.
[52] Shepherd G. Hypersensitivity reactions to chemotherapeutic drugs. Clin Rev Allergy Immunol 2003;24:253–62.
[53] Hennenfent KL, Govindan R. Novel formulations of taxanes: a review. Old wine in a new bottle? Ann Oncol 2006;17:735–49.
[54] Kenerson HL, Aicher LD, True LD, Yeung RS. Activated mammalian target of rapamycin pathway in the pathogenesis of tuberous sclerosis complex renal tumors. Cancer Res 2002;62:5645–50.
[55] Vignot S, Faivre S, Aguirre D, Raymond E. mTOR-targeted therapy of cancer with rapamycin derivatives. Ann Oncol 2005;16:525–37.
[56] González-Polo R-A, Boya P, Pauleau A-L, Jalil A, Larochette N, Souquère S, et al. The apoptosis/autophagy paradox: autophagic vacuolization before apoptotic death. J Cell Sci 2005;118:3091–102.